Advanced methodology for emulating local operating condi-tions in Proton Exchange Membrane Fuel Cells

Marine Cornet, Arnaud Morin, Jean-Philippe Poirot-Crouvezier, Yann Bultel

data

MDPI

Data Descriptor

Advanced Methodology for Emulating Local Operating Conditions in Proton Exchange Membrane Fuel Cells

Marine Cornet [1,2], Arnaud Morin [1], Jean-Philippe Poirot-Crouvezier [1] and Yann Bultel [2,*]

[1] Univ. Grenoble Alpes, CEA, LITEN, DEHT, 38000 Grenoble, France; marine.cornet@univ-grenoble-alpes.fr (M.C.); arnaud.morin@cea.fr (A.M.); jean-philippe.poirot@cea.fr (J.-P.P.-C.)
[2] Univ. Grenoble Alpes, Univ. Savoie Mont Blanc, CNRS, Grenoble INP, LEPMI, 38000 Grenoble, France
* Correspondence: yann.bultel@grenoble-inp.fr

Abstract: This work focuses on the study of operating heterogeneities on a large MEA's active surface area in a PEMFC stack. An advanced methodology is developed, aiming at the prediction of local operating conditions such as temperature, relative humidity and species concentration. A physics-based Pseudo-3D model developed under COMSOL Multiphysics allows for the observation of heterogeneities over the entire active surface area. Once predicted, these local operating conditions are experimentally emulated, thanks to a differential cell, to provide the local polarization curves and electrochemical impedance spectra. Coupling simulation and experimental, thirty-seven local operating conditions are emulated to examine the degree of correlation between local operating conditions and PEMFC cell performances. Researchers and engineers can use the polarization curves and Electrochemical Impedance Spectroscopy diagrams to fit the variables of an empirical model or to validate the results of a theoretical model.

Dataset: https://doi.org/10.57745/YLCIPH.

Dataset License: CC0

Keywords: differential cell; PEM fuel cell; local operating conditions; polarization curves; electrochemical impedance spectra

Citation: Cornet, M.; Morin, A.; Poirot-Crouvezier, J.-P.; Bultel, Y. Advanced Methodology for Emulating Local Operating Conditions in Proton Exchange Membrane Fuel Cells. *Data* **2024**, *9*, 152. https://doi.org/10.3390/data9120152

Academic Editor: Yongqing Cai

Received: 14 November 2024
Revised: 15 December 2024
Accepted: 16 December 2024
Published: 20 December 2024

1. Summary

Proton exchange membrane fuel cells (PEMFC) are now considered as a relevant solution to limit CO_2 emissions for transport and stationary applications [1,2]. The PEM fuel cell is an open system, and as such, its operation is inherently heterogeneous. Indeed, electrochemical reactions do not occur homogeneously on the active surface area. It is well accepted that operating heterogeneities over a large cell active surface area can result in a decrease of performance and durability [3].

On the one hand, investigating heterogeneities of local operating conditions on a large MEA surface area in a stack remains a key challenge as most of the parameters are difficult, or even impossible, to measure with a non-invasive device, which may perturbate the stack performance and behavior [4–7]. Moreover, experimental campaigns on a stack are money- and time-consuming when many operating conditions have to be investigated. On the other hand, PEMFC stack modelling is more accessible than experimental resources. Indeed, 3D models are able to capture the influence of the stack design and operating conditions [8,9]. Nevertheless, a full 3D stack model requires lot of numerical resources and an accurate calibration of the model based on relevant experimental data [10–14]. In this work, an advanced methodology, illustrated in Figure 1, has been developed to investigate the heterogeneities of the local operating conditions in a large MEA surface area (i.e., 250 cm^2) of a PEMFC stack.

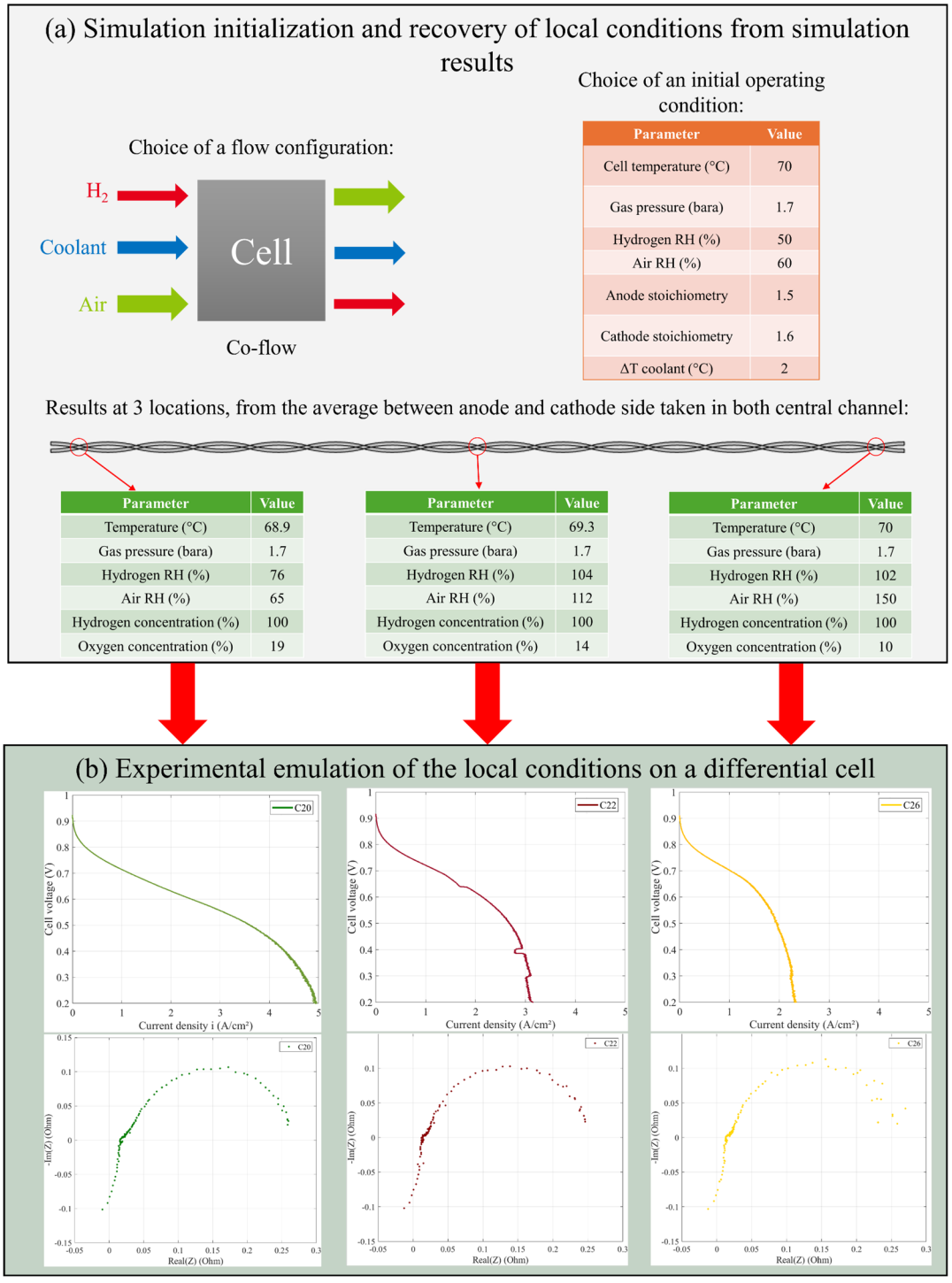

Figure 1. Illustrated methodology to (**a**) determine local conditions for each flow configuration and initial operating state, and then (**b**) emulate these conditions on a differential cell through characterization using I–V curves and EIS.

Since these local conditions cannot be measured, we decided to simulate a few operating conditions at the cell scale to recover the local conditions. Once the local conditions have been determined, they are tested with a differential cell, as it is designed to operate as homogeneously as possible and can emulate the local operation of a large cell.

To this end, the local conditions of the cell must be predicted at air inlet, middle and air outlet of the active surface area to then be experimentally emulated. These local

conditions (temperature, pressure, concentration of species) are obtained by simulation, thanks to the Pseudo-3D model with its initial calibration, and are emulated experimentally on a small cell called the differential cell. The transport equations are solved in-plane and through-plane using the Pseudo-3D approximation developed and implemented in a previous multi-physics and single-phase model by F. Nandjou et al. [15]. Indeed, to capture only the electrochemical response of the catalytic layer, without any other disturbance, the local conditions applied must be as homogeneous as possible over the studied area. These local operating conditions are then emulated thanks to a differential cell. Each local operating condition is characterized by a polarization or I-V curve and Electrochemical Impedance Spectroscopy (EIS) measurements.

2. Data Description

The different operating conditions investigated in this work are, therefore, emulated using the differential cell and protocol presented in Section 3. The methodology enables the capture of a broader range of local values for molar fractions in a dry gas, anode and cathode relative humidity, gas pressure and temperature, as gathered from three distinct regions of the simulated cell (air inlet, middle and air outlet) on both the anode and cathode sides. The thirty-seven different operating conditions are defined and referenced in Table A1 (see Appendix A). For each condition, the polarization curve is measured during the first scan with decreasing voltage from OCV down to the lower cell voltage, i.e., 0.2 V (Figure 2), and, later on, EIS measurements are performed at three different currents (Figure 3).

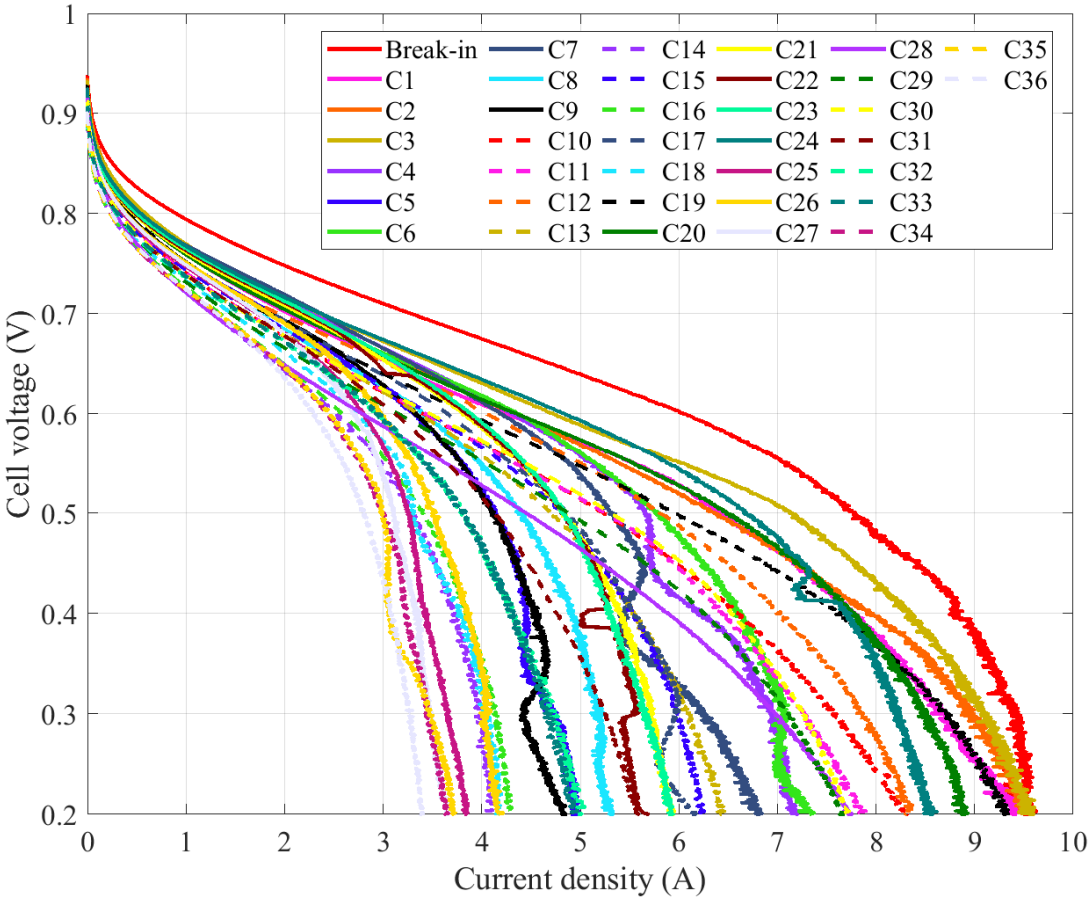

Figure 2. I–V curves for all the operating conditions.

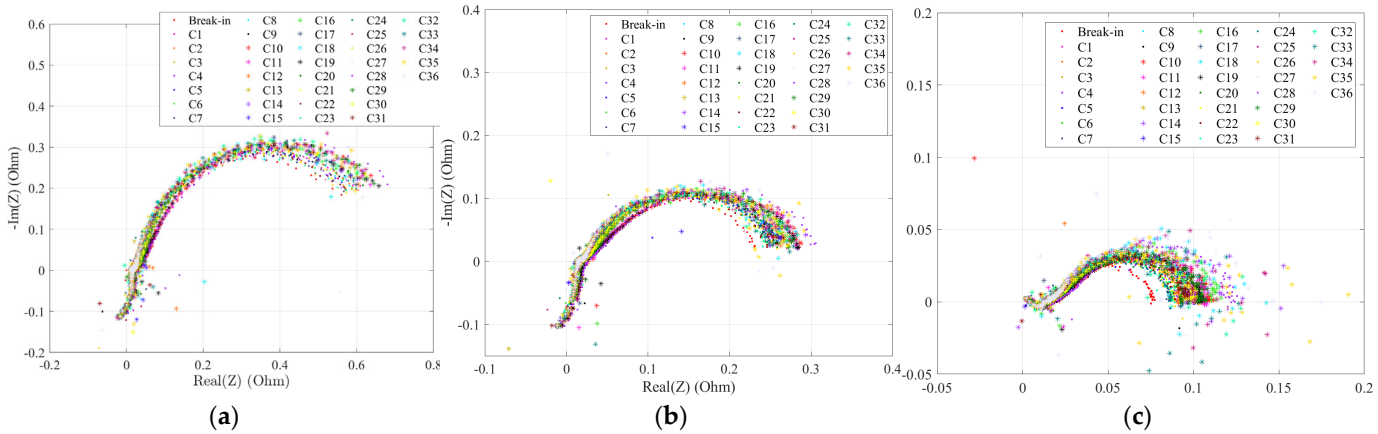

Figure 3. Electrochemical Impedance Spectra measured for all the operating conditions for the 3 different current densities (**a**) 45 mA, (**b**) 180 mA and (**c**) 900 mA.

Figure 3 shows the impedance spectra measured at low and moderate current values i.e., 45 mA, 180 mA and 900 mA (or i.e., 25 mA/cm^2, 100 mA/cm^2 and 500 mA/cm^2).

For most of the conditions tested, significant instabilities can be seen below 0.6 V in Figure 2. These instabilities can be explained by a greater production of water at high current density, causing the channels to be partially and temporarily blocked until the droplet is evacuated, allowing the reactants to pass through again.

Each file contains either data from the polarization curve or the electrochemical impedance spectrum:

- Break-in_IV and CX_IV. This file contains the experimental raw data of the polarization curve of the operating condition X. All raw data files are organized with the same structure: the first column provides the current (A) and the second one the corresponding cell voltage (V);
- Break-in_EIS and CX_EIS. This file contains the experimental raw data of the impedance spectrum of the operating condition X at low (i.e., 45 mA, 180 mA) or medium (i.e., 900 mA) currents. All raw data files are organized with the same structure: The first and second columns refer, respectively, to current (A) and cell voltage (V). The columns 3, 4 and 5 report the frequency (Hz), the real(Z) (Ω) and -Im(Z) (Ω), respectively. Finally, columns 6 and 7 give the module (Ω) and the phase angle (°), respectively.

3. Methods

3.1. Emulated Local Operation Conditions

To obtain a large variety of local operating conditions, three different flow configurations are computed, as represented in Figure 4: counter-flow with the coolant flowing in the same direction as the hydrogen, co-flow and, finally, counter-flow with the coolant flowing in the same direction as the air. Whatever the flow configuration, four distinct operating conditions representative of automotive application points are simulated using the Pseudo-3D model [15]. These conditions include a coolant outlet temperature ranging from 60 to 80 °C, gas pressures between 1.1 bara and 2 bara, and relative humidity levels of 50% for the anode and 60% for the cathode. These four different operating conditions, considered at the cell inlet, are detailed in Table 1. Local values of molar fractions in a dry gas, anode and cathode relative humidity, gas pressure and temperature are extracted at the air inlet, middle and air outlet from simulations at the cathode and anode, providing 36 local conditions to be emulated. An additional operating condition is included in the experimental protocol, supplementing the thirty-six existing conditions. This additional condition is repeated at the start and end of the test to provide brief cell conditioning and ensure reproducibility. The thirty-seven distinct operating conditions are presented in Table A1.

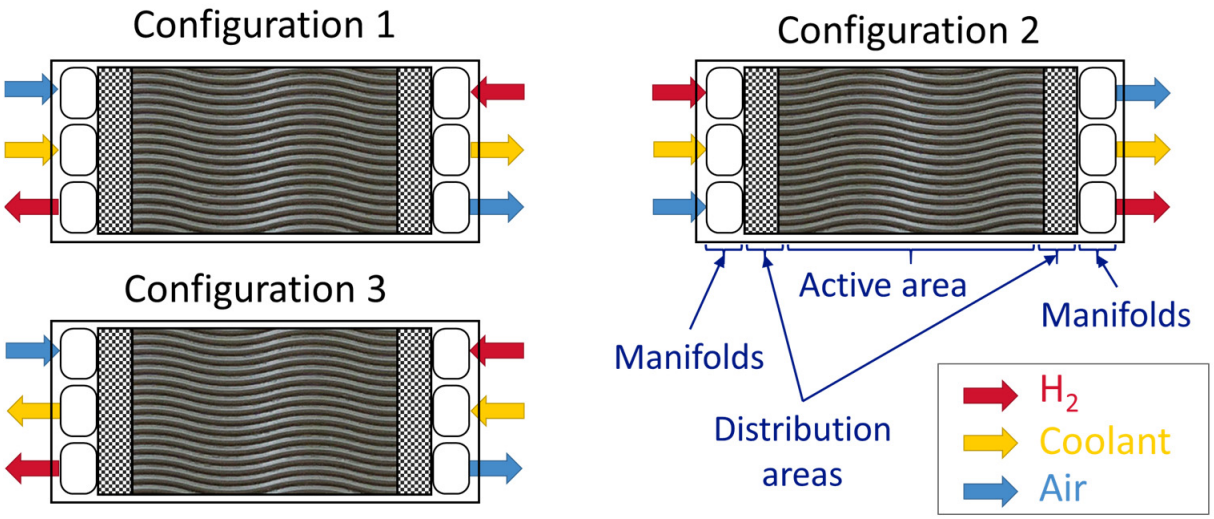

Figure 4. Representation of the three flow configurations simulated with the Pseudo-3D model.

Table 1. Operating conditions simulated with the Pseudo-3D model to obtain local conditions to emulate with a differential cell.

Type of Power Output	High (1.14 A/cm^2)	Nominal (0.7 A/cm^2)	Medium (0.4 A/cm^2)	Low (0.2 A/cm^2)
Cell temperature (°C)	80	80	70	60
Gas pressure (bara)	2	1.5	1.7	1.1
H_2 relative humidity (%)	50	50	50	50
Air relative humidity (%)	60	60	60	60
H_2 stoichiometry	1.5	1.5	1.5	1.5
Air stoichiometry	1.6	1.6	1.6	1.6
ΔT cooling (°C)	5	5	2	2

3.2. Data Acquisition

3.2.1. Materials

In this work, a differential cell is used to emulate the thirty-seven operating conditions that can be observed locally on larger cells. A differential or zero gradient PEM fuel cell is typically a small cell designed to ensure homogeneous in-plane operation, thereby enabling the application of well-controlled operating conditions [16]. The CEA-designed cell utilized in this study exhibits an active surface area of 1.8 cm^2. It features 32 parallel straight gas channels, machined in graphite plates, with a width of 250 µm and a depth of 400 µm, separated by a rib of 250 µm width. Figure 5a shows a photo of the differential cell during assembly. It is designed with narrow ribs and channels and a small distance between channels inlet and outlet. These small dimensions enable a better distribution of mechanical stress and as little pressure drop as possible in the channels. This design, therefore, limits heterogeneities on the rib/channel scale, as well as between the inlet and outlet of the channels. In addition, this cell is used with high fixed gas flow rates of 45 NL/h at the anode and 113 NL/h at the cathode. These flow rates correspond to a stoichiometry of 30 at 2 A/cm^2. The reactants consumed and the water produced are, therefore, negligible compared with what enters the cell. The pressure drop induced by these flow rates between the inlet and the outlet of the active area is lower than 50 mbar for both reactants. Therefore, the concentrations of water and reactants remain practically constant between the inlet and outlet of the channels. This ensures maximum uniformity in cell operation.

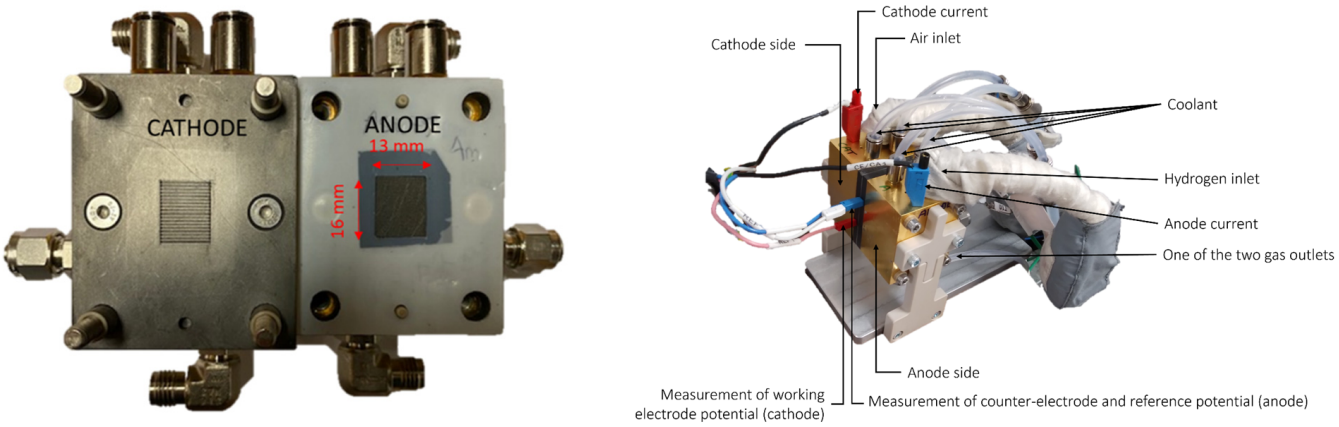

(**a**) (**b**)

Figure 5. (**a**) Differential cell during assembly and (**b**) differential cell during operation on the test bench.

The MEA used features a commercial Catalyst Coated Membrane (CCM), specifically the GORE® PRIMEA® MEA, comprising a 15 µm reinforced membrane and electrodes with platinum loadings of 0.1 mg/cm^2 for the anode and 0.4 mg/cm^2 for the cathode. A commercial GDL Sigracet 22BB from SGL Carbon, with an uncompressed thickness of 215 µm, is employed on both sides. This assembly is placed in the cell, enclosed by a 150 µm thick PTFE hard stop gasket, to regulate the final thickness of the compressed GDL, ensuring a 30% compression level.

The differential cell is tested using an in-house test bench, which controls the operating conditions. It enables feeding of the cell with dry or humidified H_2, O_2, N_2 and air. It is also possible to combine various types of gases, including both dry and wet gases, while maintaining controlled flow rates from 0.5 NL/h to 200 NL/h. The differential cell can be fed with diluted oxygen in nitrogen at various molar fractions. The gases are humidified by passing through temperature-controlled bubblers, achieving the desired relative humidity level. Lastly, the test bench manages a thermostatic bath that uses deionized water to regulate the operating temperature of the cell. The differential cell on the test bench is presented in Figure 5b. The cell voltage is regulated using a BioLogic SP-150 potentiostat equipped with a ±20 A booster (adjustable from −20 to +20 V), combined with EC-Lab® control and analysis software. The characteristics of the potentiostat are detailed in [17]. Once the test bench stabilizes at the desired operating conditions, the potentiostat initiates the characterization sequence described in the next sub-section.

3.2.2. Cell Characterization Description

The chosen cell characterization protocol begins with a measurement of the available platinum surface area by cyclic voltammetry (CV) at the beginning of the test (BoT), which corresponds to the cell's beginning of life (BoL), followed by a break-in or conditioning of the cell. The protocol continues with a sequence of characterization repeated for each operating condition. This sequence includes a short conditioning period, to mitigate cell history effect as much as possible, followed by the measurement of the electrochemical response of the cell to a voltage ramp (Polarization or I-V curve), and is finalized by several measurements of electrochemical impedance spectra. After applying this characterization sequence for all operating conditions, the break-in process is repeated. Finally, repeating the break-in process at the end of test (EoT) of the cell enables us to assess potential damage to the sample.

Break-in is important for complete activation of the CCM in the MEA to reach nominal performance. A voltage scan from OCV (0.95 V) to 0.1 V with a scan rate of 100 mV/s followed by a constant voltage period of 60 s at 0.1 V is applied. This cycle is repeated 15 times to complete the break-in process, both at the initial cell startup and before a

polarization curve measurement is carried out. Cyclic voltammetry is a commonly employed technique for the characterization of fuel cell catalyst redox properties. In this electrochemical technique, the cell is fed with H_2 at the anode (reference/counter electrode) and N_2 at the cathode (working electrode) while the cell's potential is oscillated between two specified limits and the current is recorded. The cell's voltage cycles between 0.090 V and 1.2 V. That measurement is performed several times at 100 mV/s. It enables the calculation of the electrochemical surface area (ECSA), equal to 216 cm^2 Pt for the cathode. The dataset considered for data processing is that of the last cycle, because the cell's catalyst has likely been depolluted by the previous cycles. The operating conditions under which these processes take place are detailed in Table 2.

Table 2. Operating condition of the break-in phase and for the cyclic voltammetry measurement of a differential cell.

	Break-In	**CV**
Cell temperature (°C)	80	30
Gas pressure anode/cathode (bar absolute)	2.5/2.3	1.5/1.5
Relative Humidity anode/cathode (%)	95/95	110/110
Gas flow rate anode/cathode (NL/h)	45/113	50/50
Dry gas concentration H_2/O_2 (%)	100/21	100/0

For each condition of Table A1, the polarization curve of the differential cell is obtained by measuring the current produced by the cell for a voltage ramp, back and forth. The ramp goes from OCV to 0.2 V and back at a sweep rate of 1 mV/s.

The impedance spectra are measured at 3 different currents, i.e., 45, 180 and 900 mA. For each current, the amplitude of the small current variation during the measurement is of 2 mA, 5 mA and 10 mA, respectively. The frequency range of the measurement is 1 Hz–200 KHz. This frequency range is divided into 20 points per decade in logarithmic spacing and two measurements of the impedance are taken per frequency.

3.3. Validation

To ensure that the performance measured is that of a healthy cell and that the protocol is not degrading, we compared measurements taken at the start and end of the test. The comparison of the polarization curve for the same condition at the beginning and end of the test is shown in Figure 6a. This condition is the one applied during the cell break-in phase, as it is the first operating condition tested. We can observe that the I-V measurements taken at the beginning and end of test are very similar and that the cell is not degraded by the protocol used.

Moreover, two samples of the same MEA were tested using the protocol described previously to evaluate its reproducibility. The results shown above are those obtained from measurements on the first cell (Cell #1). The second sample (Cell #2) was taken from the same batch of CCM and GDL sheets and assembled in the same differential cell hardware. As shown in Figure 6b, the two curves almost overlap up to 0.6 V. Beyond that, the curves diverge slightly up to 0.5 V, after which the gap widens. The section of the curve at high current density, where the curves diverge, corresponds to mass transport effects. This section of the curve is highly sensitive to the presence of water droplets in the cell during the test and to GDL heterogeneities.

The superposition of the curves up to 0.6 V appears to provide sufficient evidence to conclude that the protocol is reproducible.

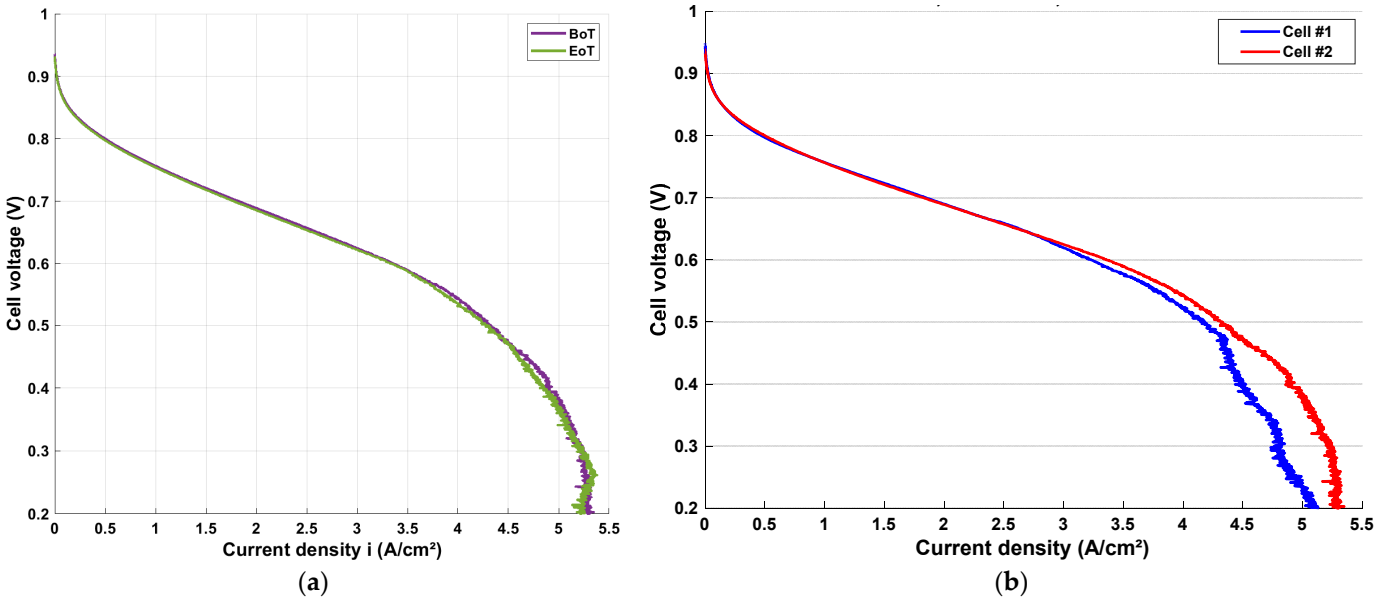

Figure 6. Comparison of polarizations curves (**a**) at the BoT and EoT for the same sample and (**b**) measured for the two samples of MEA#1 in the same condition (C0): 80 °C, anode/cathode relative humidity (RH) 95/95%, anode/cathode gas pressure 2.5/2.3 bara.

4. User Notes

A major challenge lies in analyzing the heterogeneities of local operating conditions across a large MEA active surface area within a stack. On one hand, conducting experimental campaigns on a stack is both costly and time-intensive, particularly when numerous operating conditions must be evaluated. On the other hand, PEMFC stack modeling offers greater accessibility compared to experimental methods. However, calibrating PEMFC models remains a critical hurdle. Although some MEA properties can be obtained from the manufacturer or experimental data, the electrochemical response of the model must be fine-tuned to reflect the actual behavior of the selected MEA. Indeed, the voltage–current relationship incorporated into models is typically derived by fitting the electrochemical response of a PEMFC under a limited set of operating conditions.

This paper presents an advanced methodology for emulating local operating conditions across a large MEA surface area using experimental measurements from a differential cell. Polarization curves and Electrochemical Impedance Spectra were obtained over a wide range of parameters, including molar fractions in dry gas, anode and cathode relative humidity, gas pressure, and temperature, effectively simulating local conditions up to 2 A/cm^2. To ensure that only the electrochemical response of the MEA was captured, free from external disturbances, a differential cell was employed to maintain the most uniform local conditions possible over the studied area.

The data provided herein have been useful in fitting a cell voltage law to the local electrochemical behavior on a large MEA surface area in a stack [18]. In this latter study, these experimental data were used to fit the eight β_i coefficients of a semi-empirical cell voltage law to obtain more accurate simulation results in a wide range of operating conditions. Experimental and simulated polarization curves were also compared in ref. [18], showing a maximum deviation of 10.4%. Note that the highest current densities are the most challenging to model, as they represent the diffusion limits and are, therefore, governed by mass transport processes. Figure 7 recaps different steps used for cell voltage calibration. Once calibrated, the Pseudo-3D model was used for a sensitivity study of operating heterogeneities over a wide range of operating conditions. Note that 108 operating conditions were selected according to a full factorial design of experiment featuring variation in coolant outlet temperature, coolant temperature gradient and anode/cathode gas RH in order to choose which ones must be experimentally tested.

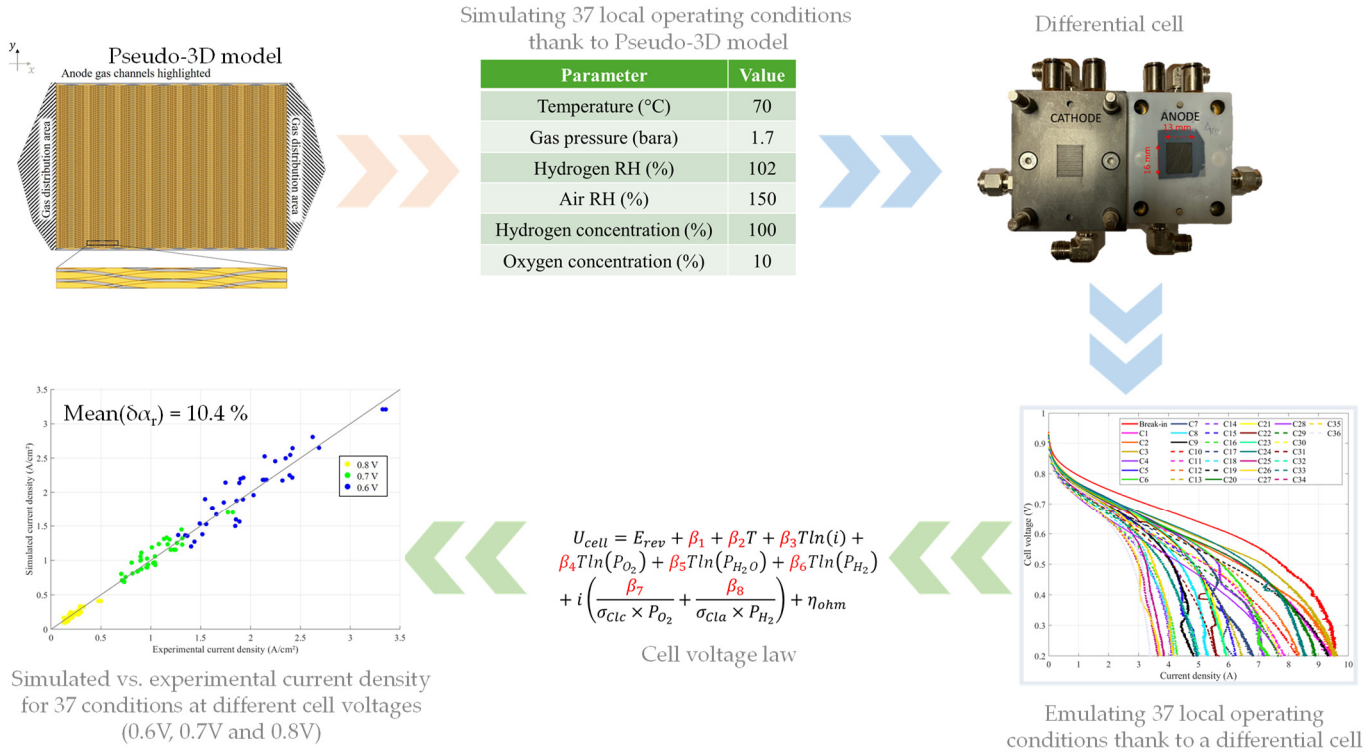

Figure 7. Advanced methodology for emulating local operating conditions on large MEA surface area.

Author Contributions: Conceptualization, M.C., A.M., J.-P.P.-C. and Y.B.; methodology, M.C., A.M. and J.-P.P.-C.; validation, M.C., A.M. and J.-P.P.-C.; formal analysis, M.C.; investigation, M.C.; resources, A.M. and J.-P.P.-C.; data curation, M.C. and Y.B.; writing—original draft preparation, Y.B.; writing—review and editing, Y.B., M.C. and J.-P.P.-C. All authors have read and agreed to the published version of the manuscript.

Funding: This research received no external funding.

Data Availability Statement: The original data presented in the study are openly available on https://doi.org/10.57745/YLCIPH.

Conflicts of Interest: The authors declare no conflict of interest.

Appendix A

Table A1. Thirty-seven operating conditions tested with the differential cell (the H_2 molar fraction in dry gas is 100% for all conditions).

Name	Cell Temperature (°C)	Gas Pressure Anode/Cathode (Bar Absolute)	Relative Humidity (RH) (%)		Molar Fraction in Dry Gas (%)
			Anode	Cathode	O_2 (Cathode)
C1	84	2.0	75	61	19
C2	79		75	62	19
C3	79		91	73	19
C4	82		85	104	14
C5	83		82	113	9
C6	82		84	94	14
C7	80		90	107	13
C8	83		71	117	10
C9	77		88	143	9

Table A1. *Cont.*

Name	Cell Temperature (°C)	Gas Pressure Anode/Cathode (Bar Absolute)	Relative Humidity (RH) (%)		Molar Fraction in Dry Gas (%)
			Anode	Cathode	O_2 (Cathode)
C10	78	1.7	72	66	20
C11	82		83	63	19
C12	78		100	75	19
C13	80		91	85	14
C14	83		77	112	9
C15	82		91	102	14
C16	82		87	103	9
C17	79		96	105	14
C18	77		95	137	9
C19	69	1.5	77	66	20
C20	71		100	74	19
C21	70		104	113	14
C22	70		104	134	14
C23	70		106	137	14
C24	69		108	79	19
C25	71		102	151	9
C26	71		101	161	10
C27	69		110	177	9
C28	59	1.1	75	68	20
C29	61		99	76	19
C30	59		106	82	20
C31	60		107	112	15
C32	60		107	137	14
C33	59		109	140	14
C34	60		104	153	10
C35	63		104	170	10
C36	58		114	185	10
C37	80	2.5/2.3	95	95	21

References

1. European Hydrogen Observatory. Hydrogen Value Chains | European Hydrogen Observatory. September 2023. Available online: https://observatory.clean-hydrogen.europa.eu/sites/default/files/2023-09/Factsheets-Hydrogen%20value%20chain%20.pdf (accessed on 10 March 2023).
2. U.S. Department of Energy. Comparison of Fuel Cell Technologies. Available online: https://www.energy.gov/eere/fuelcells/articles/comparison-fuel-cell-technologies-fact-sheet (accessed on 8 April 2024).
3. Lochner, T.; Hallitzky, L.; Perchthaler, M.; Obermaier, M.; Sabawa, J.; Enz, S.; Bandarenka, A.S. Local Degradation Effects in Automotive Size Membrane Electrode Assemblies under Realistic Operating Conditions. *Appl. Energy* **2020**, *260*, 114291. [CrossRef]
4. Pérez, L.C.; Brandão, L.; Sousa, J.M.; Mendes, A. Segmented polymer electrolyte membrane fuel cells—A review. *Renew. Sustain. Energy Rev.* **2011**, *15*, 169–185. [CrossRef]
5. Fink, C.; Fouquet, N. Three-dimensional simulation of polymer electrolyte membrane fuel cells with experimental validation. *Electrochim. Acta* **2011**, *56*, 10820–10831. [CrossRef]
6. Lobato, J.; Canizares, P.; Rodrigo, M.; Pinar, F.; Ubeda, D. Study of flow channel geometry using current distribution measurement in a high temperature polymer electrolyte membrane fuel cell. *J. Power Sources* **2011**, *196*, 4209–4217. [CrossRef]
7. Toharias, B.; Suárez, C.; Iranzo, A.; Salva, M.; Rosa, F. Dataset and Measurements from a Current Density Sensor during Experimental Testing of Dynamic Load Cycling for a Parallel-Serpentine Design of a Proton Exchange Membrane Fuel Cell. *Data Brief* **2024**, *54*, 110392. [CrossRef] [PubMed]
8. Zhang, G.; Wu, J.; Wang, Y.; Yin, Y.; Jiao, K. Investigation of current density spatial distribution in PEM fuel cells using a comprehensively validated multi-phase non-isothermal model. *Int. J. Heat Mass Transf.* **2020**, *150*, 119294. [CrossRef]

9. Baca, M.; Travis, R.; Bang, M. Three-dimensional, single-phase, non-isothermal CFD model of a PEM fuel cell. *J. Power Sources* **2008**, *178*, 269–281. [CrossRef]
10. Arif, M.; Cheung, S.C.P.; Andrews, J. Different Approaches Used for Modeling and Simulation of Polymer Electrolyte Membrane Fuel Cells: A Review. *Energy Fuels* **2020**, *34*, 11897–11915. [CrossRef]
11. Rizvandi, O.B.; Yesilyurt, S. A transient Pseudo-3D model of the PEM fuel cell for the analysis of dead-ended anode and anode bleeding operation modes. *Electrochim. Acta* **2019**, *324*, 134866. [CrossRef]
12. Yin, C.; Yang, H.; Liu, Y.; Wen, X.; Xie, G.; Wang, R.; Tan, H. Numerical and experimental investigations on internal humidifying designs for proton exchange membrane fuel cell stack. *Appl. Energy* **2023**, *348*, 121543. [CrossRef]
13. Zou, Y.; Hua, S.; Wu, H.; Chen, C.; Wei, Z.; Hu, Z.; Lei, Y.; Wang, J.; Zhou, D. Design of a New Single-Cell Flow Field Based on the Multi-Physical Coupling Simulation for PEMFC Durability. *Energies* **2023**, *16*, 5932. [CrossRef]
14. Rahmani, E.; Moradi, T.; Ghandehariun, S.; Naterer, G.F.; Ranjbar, A. Enhanced mass transfer and water discharge in a proton exchange membrane fuel cell with a raccoon channel flow field. *Energy* **2023**, *264*, 126115. [CrossRef]
15. Nandjou, F.; Poirot-Crouvezier, J.-P.; Chandesris, M.; Bultel, Y. A pseudo-3D model to investigate heat and water transport in large area PEM fuel cells—Part 1: Model development and validation. *Int. J. Hydrogen Energy* **2016**, *41*, 15545–15561. [CrossRef]
16. Riasse, R.; Lafforgue, C.; Vandenberghe, F.; Micoud, F.; Morin, A.; Arenz, M.; Durst, J.; Chatenet, M. Benchmarking proton exchange membrane fuel cell cathode catalyst at high current density: A comparison between the rotating disk electrode, the gas diffusion electrode and differential cell. *J. Power Sources* **2023**, *556*, 232491. [CrossRef]
17. Available online: https://my.biologic.net/products/sp-150e_potentiostat/ (accessed on 11 March 2024).
18. Cornet, M.; Poirot-Crouvezier, J.-P.; Schott, P.; Kawka, S.; Morin, A.; Bultel, Y. Advanced Methodology for Simulating Local Operating Conditions in Large Fuel Cells Based on a Spatially Averaged Pseudo-3D Model. *J. Electrochem. Soc.* **2024**, *171*, 104514. [CrossRef]